## REPORT DOCUMENTATION PAGE

Form Approved OMB No. 0704-0188

Public reporting burden for this collection of information is estimated to average 1 hour per response, including the time for reviewing instructions, searching existing data sources, gathering and maintaining the data needed, and completing and reviewing the collection of information. Send comments regarding this burden estimate or any other aspect of this collection of information, including suggestions for reducing this burden. To Washington Headquarters Services, Directorate for information Operations and Reports, 1215 Jefferson Davis Highway, Suite 1204, Arlington, VA 22202-4302, and to the Office of Management and Budget, Paperwork Reduction Project (0704-0188), Washington, DC 20503.

1. AGENCY USE ONLY (Leave blank)	2. REPORT DATE	3. REPORT TYPE AND	DATES COVERED	
	9-15-95	Final Report 3-		
4. TITLE AND SUBTITLE		5	. FUNDING NUMBERS	
Reversible and Selective	Fiber Optic Hydraz	<del></del>	hillips Labora	
Detector		1 (	(FMBD) SBIR Pha	se I
			Contract No.	
6. AUTHOR(S)		E	'29601-95 <b>-</b> C-012	8
M. Schwartz, J.D. Young,	and A.F. Sammells		•	
<u>pointage</u> , con a samp,				
TO WAST	C) AND ADDRESS(ES)		. PERFORMING ORGA	NIZATION
7. PERFORMING ORGANIZATION NAME	(2) אום אסטעבפפונפון		REPORT NUMBER	
Blanca Degenwah Ing			Final Report	
Eltron Research, Inc. 2830 Wilderness Place		,	Project 076	
Boulder, CO 80301			110,000 070	
Bourder, co octor	•			
9. SPONSORING/MONITORING AGENCY	NAME(S) AND ADDRESS(ES)	1	O. SPONSORING / MON	
Phillips Laboratory			AGENCY REPORT N	UMBEK
Directorate of Contract	ing			
2251 Maxwell Avenue SE	1			
Kirtland AFB, NM 87117-	5772	19991117	7 127	
		17771111	וכו	
11. SUPPLEMENTARY NOTES		1777		
				× .
		1		
12a. DISTRIBUTION / AVAILABILITY STAT	EMENT		2b. DISTRIBUTION CO	DE
12a. DISTRIBUTION / NAMICABILITY STATE	Lincin	,		
Unlimited Distribution				
OHITMITEE DISCIDUCION				
13. ABSTRACT (Maximum 200 words)				1
The project object	tive was directed	d towards devel	opment and su	ibsequent
commercialization, for	r dual use appli	cations, of a c	listributed m	nultisite
fiber optic chemical	sensor technol	logy for achie	ving the re	ear time
monitoring of unsymme	trical dimethylh	ydrazine (UDMH	) and its co	ongeners,
monomethylhydrazine	(MME) and hyd	razine (H) d	lown to th	
concentration level.	Selective detect	tion of hydrazi	nes was peri	cormed by
monitoring absorbance	changes via evan	escent wave int	eraction at 1	rue riber
optic surface. During	performance of	this program th	ese nydrazine	s species
were reversibly detec	ted at concentr	ation levels d	OWIL CO TOPP.	o tibor
using triphenylmethan	e dyes immobiliz	ed onto the sur	riace of sill . Experimen	ted liber
optic sensors operati	ng in the evanes	scent wave mode		
demonstrated that a sp	atial resolution	for liber option	nis indicate	d that a
several tens of meter	rs can easily be			
distributed network fo	r the reversible	detection of t	race Hydrazii	nes coura
be fabricated using s	tandard electroo	ptical componer	ILS.	~
14. SUBJECT TERMS		- Bibar Ontin Com	15. NUMBER	OF PAGES
Multisite Detection, Reversible Fiber Optic Se Selectivity, Hydrazine		e riber Optic Sens	16. PRICE CO	
Selectivity	, nydrazine		IO. PRICE CO	π
	CECURITY CLASSICS FICE	19. SECURITY CLASSIFICA	TION 20 LIMITATI	ON OF ABSTRACT
	SECURITY CLASSIFICATION OF THIS PAGE	OF ABSTRACT	20. CIVITATI	OIL OI ADDINACT

Unclassified NSN 7540-01-280-5500

OF REPORT

Unclassified

Unclassified

Standard Form 298 (Rev. 2-89) Prescribed by ANSI Std (39-18

None

# TABLE OF CONTENTS

	<u>.</u>	<u>'age</u>
I.	INTRODUCTION	2
II.	PHASE I TECHNICAL OBJECTIVES	4
ш.	WORK PERFORMED AND RESULTS OBTAINED	4
	Task 1 Evaluation of Spectral Properties of Selected Triphenylmethane Dyes to Low Concentrations of Hydrazines	4
	a. Experimental	7
	b. Sample Preparation	8
	c. Experimental Results	9
	Task 2 Performance Characterization of Immobilized Triphenylmethane Dyes on Fiber Optics for the Reversible Detection of Hydrazines	10
	a. Optical Response to Hydrazine, 1,1'-Dimethylhydrazine and Monomethylhydrazine	10
	b. Evaluating Ammonia as a Potential Interferant for Hydrazine Detection	19
	c. Evaluating Water as a Potential Interferant for Hydrazine Detection	24
	d. Towards Distributed Fiber Optic Sensor Measurements	26
IV.	SUMMARY OF PHASE I RESULTS	27
v.	ESTIMATE OF TECHNICAL FEASIBILITY	28
A.	Background	28
В.	Fiber Optic Sensor Network Architecture	30
C.	Power Budget and Number of Sites for Detection	31
n	Spatial Desolution	32

# TABLE OF CONTENTS (cont'd)

		<u>Page</u>
VI.	RELATIONSHIP WITH FUTURE RESEARCH OR R&D EFFORTS	32
VII.	POTENTIAL POST APPLICATIONS	35
VIII.	REFERENCES	38

# LIST OF FIGURES

		<u>Page</u>
Figure 1.	Reaction shown between UDMH and the triphenylmethane dye crystal violet to give a colorless adduct which forms the basis of the subject fiber optic sensor technology.	3
Figure 2.	Schematic configuration for fiber optical detection (a) and generation of the evanescent wave at an interface between two optical media (b) used in this program for reversible detection of hydrazines.	5
Figure 3.	Schematic of experimental arrangement used during Phase I for initially screening the optical response of triphenylmethane dyes immobilized onto glass slides.	7
Figure 4.	Schematic of test chamber incorporating glass slide containing immobilized triphenylmethane dye for hydrazine detection.	8
Figure 5.	Circuitry used in conjunction with the PIN photodetector to detect signals from the chemical transducer dye when exposed to hydrazines.	9
Figure 6.	Response of a glass slide coated with crystal violet towards 100ppb hydrazine in air at 600nm.	10
Figure 7.	Schematic of sample chamber used for hydrazine detection in silica fiber optic sensors operating in the evanescent wave mode.	11
Figure 8.	Schematic of experimental arrangement used to detect hydrazine in the absorption mode by coating the sensing dye on the distal end of the silica fiber optic.	12
Figure 9.	Response towards 10ppm hydrazine in air in the absorption mode of the silica fiber optic with its distal end coated with crystal violet.	12
Figure 10.	Response towards 1ppm hydrazine in air in the absorption mode of a silica fiber optic with its distal end coated with crystal violet.	13
Figure 11.	Schematic of revised experimental fiber optic sensor configuration used to detect hydrazine in air at concentrations <1ppm.	13
Figure 12.	Comparative molecular structures of crystal violet and malachite green.	14
Figure 13.	Reaction scheme used during Phase I to convert malachite green carbinol hydrochloride into malachite green chloride.	15

# LIST OF FIGURES (Cont'd).

		<u>Page</u>
Figure 14.	Response towards 10-35ppb hydrazine in air of a sensor based on malachite green in the evanescent wave mode.	16
Figure 15.	Response of a malachite green based fiber optic sensor to 1ppm UDMH in air operating in the evanescent wave mode. The light source was a laser diode operating at 635nm.	16
Figure 16.	Response of a malachite green based sensor to 50ppb UDMH in air operating in the evanescent wave mode. The light source was a laser diode operating at 635nm.	17
Figure 17.	Response of a malachite green based sensor to 81ppb MMH in air operating at the evanescent wave mode. The light source was a laser diode operating at 635nm.	17
Figure 18.	Response towards 40ppm hydrazine of a sensor prepared by evaporation of crystal violet onto a silica optical fiber. This test was performed three days after preparation.	18
Figure 19.	Response towards 40ppm hydrazine of sensor used in Figure 18 after four days of testing.	18
Figure 20.	Response towards 40ppm hydrazine of sensor shown in Figure 19 after six days of testing.	19
Figure 21.	Response of a malachite green based fiber optic sensor operating in the evanescent wave mode towards 20ppb $N_2H_4$ in air.	20
Figure 22.	Response of a malachite green based fiber optic sensor operating in the evanescent wave mode towards 1ppm $NH_3$ in air.	20
Figure 23.	Response of a malachite green based fiber optic sensor operating in the evanescent wave mode towards $100 \text{ppb NH}_3$ in air.	21
Figure 24.	Response of a malachite green based fiber optic sensor operating in the evanescent wave mode towards 50ppm $NH_3$ in air.	22
Figure 25.	Wavelength response dependence of a malachite green based fiber optic sensor operating in the evanescent wave mode towards 500ppb $N_2H_4$ and 10ppb $NH_3$ in air. Intensities are relative to the sensor in air.	22

# LIST OF FIGURES (Cont'd).

		<u>Page</u>
Figure 26.	Wavelength response dependence of a malachite green based fiber optic sensor operating in the evanescent wave mode towards 500ppb $N_2H_4$ and 10ppm $NH_3$ in air. Intensities are relative to the fiber optic sensor in air.	23
Figure 27.	Wavelength dependence of the response of a malachite green fiber optic sensor operating in the evanescent wave mode towards 500ppb $N_2H_4$ , 10ppm $NH_3$ , 84ppb MMH and 30ppb UDMH. Intensities are relative to the fiber optic sensor in air.	24
Figure 28.	Response of a crystal-violet-coated silica optical fiber to 3000ppm water vapor in air at 635nm in the evanescent wave mode.	25
Figure 29.	Response of an uncoated silica optical fiber to 3000ppm water vapor in air at 635nm in the evanescent wave mode.	25
Figure 30.	Experimental arrangement showing laser diode pulsing and detector circuitry for detecting narrow light pulses required to obtain spatial resolution in a distributed fiber optic network for determining atmospheric hydrazine concentrations.	26
Figure 31.	Oscilloscope traces showing detection of delayed light pulse which corresponds to spatial resolution of ~7.5m.	27
Figure 32.	Six site linear array network for use with back reflected fiber optic geometries showing the time sequence converting the spatial domain to the time domain.	31
Figure 33.	Six site linear array network showing the required coupling ratios each ensuring that equal light intensities reach each site.	32
Figure 34.	Schematic illustration showing the use of a fiber optic coil as one possible option for increasing the light path to achieve a narrower site spatial resolution.	33
Figure 35.	First generation sensor head design under commercial development at Eltron incorporating fiber optic signal transmission.	35
Figure 36.	Schematic of fiber optic communication link strategy between sensor and home base unit for "first generation" technology currently being implemented at Eltron.	36

#### I. INTRODUCTION

This program was directed towards the development and subsequent commercialization, for dual use applications, of a distributed multisite fiber optic chemical sensor technology for achieving the real time monitoring of unsymmetrical dimethylhydrazine (UDMH) and its congeners, monomethylhydrazine (MMH) and hydrazine, down to the 10ppb concentration level. As will become evident in this document, reversible detection of hydrazines down to this concentration level was successfully achieved during performance of the Phase I program using this general approach.

Fiber optic chemical sensor technology being developed in this program relies upon the previously identified<sup>1-3</sup> reversible chemical bleaching of selected triphenylmethane dyes. During the Phase I investigation triphenylmethane dyes were immobilized onto the surface of silica optical fibers. Multiple internal reflections occurred along the fiber optic surface as an incident probe beam, of an appropriate wavelength, proceeded down the optical fiber core. Interaction of this probe beam with the surface-immobilized dye allowed for the reversible detection of hydrazines over the desired concentration range.

Prior to the inception of this program hydrazines had been shown to reversibly react with the central carbon atom of triphenylmethane dyes forming Lewis acid-base adducts.<sup>1-3</sup> Formation of these adducts results in chemically bleaching these intensely colored dyes to give, upon complete saturation, colorless intermediates. Subsequent removal of the hydrazine, for a completely reversible system, shifts the equilibrium back to the free triphenylmethane dye, restoring the initial intense coloration. This is illustrated by interaction between crystal violet and UDMH in Figure 1. While technical emphasis was placed upon hydrazine during this program, reversible optical responses were found for all three respective trace species, UDMH, MMH and hydrazine in the atmosphere, upon adduct formation with immobilized triphenylmethane dyes on fiber optic substrates. Since this program resulted in the identification of fiber optic sensor technology compatible with the reversible detection of hydrazines originating from rocket propellants and Air Force fighter aircraft, it will be compatible for eventual commercialization. Distributed fiber optic technology to emerge during performance of this program will also find commercial application for both indoor air quality monitoring and distributed toxic atmospheric gas detection systems. This technology will consequently have utility both by the Air Force and the private sector, corresponding to a dual use application.

Prior to the inception of this program fiber optic chemical sensors (FOCS) for detecting hypergolic vapors had been a relatively unexplored area. Work performed at Eltron Research, Inc. (Eltron) and by others had however suggested that the approach may provide for low cost, reversible, distributed sensor arrays. Furthermore, previous work<sup>4</sup> with an unoptimized oxazine based optical waveguide sensor had demonstrated hydrazine detection down to the 10ppm concentration level.

Our initial literature survey relating to hydrazine sensors<sup>5-13</sup> suggested that several technical approaches have the potential for reversibly detecting hydrazine vapors in the ppb concentration range. Each technique however had intrinsic limitations. These detection strategies <sup>5,6,8-10</sup> included electrochemical, chemiluminescent, photoacoustic and chemiresistor

$$N(CH_3)_2$$
+  $N_2H_4$ 
-  $C$ 
-  $N_2H_4$ 
-  $N(CH_3)_2$ 

Figure 1. Reaction shown between UDMH and the triphenylmethane dye crystal violet to give a colorless adduct which forms the basis of the subject fiber optic sensor technology.

techniques. Electrochemical detection of UDMH and its congeners had been based on measuring hydrazine oxidation currents at noble metal anodes. This had been performed in both aqueous (23% KOH) and nonaqueous (n-methyl-2-pyrolidone) electrolytes at the respective electrodes Au, Pb, In, and Rh. Hydrazine detection limits at Teflon bonded gold electrodes in 23% KOH were found to be at least 20ppb. However direct chemical reaction between aqueous KOH and atmospheric CO<sub>2</sub> were found to limit sensor lifetime to ~21 days. In comparison, electrochemical sensors using organic electrolytes suffer from electrolyte evaporation and lower sensitivity since gas diffusion electrodes (where a stabilized gas/liquid interface can be achieved conveniently with aqueous electrolytes) are not practical.

Chemiluminescence based hydrazine sensors have also achieved low ppb detection levels (~15ppb).<sup>9</sup> In this detection strategy, ozone was initially reacted with hydrazine in the presence of oxygen with resulting chemiluminescence being measured at 400nm in the case of MMH. However a major limitation of this approach was the requirement for a continuous ozone source and the sensor possessing an intrinsic sensitivity to trace NO<sub>x</sub>. Detection of hydrazines had also been performed by the complementary use of a CO<sub>2</sub> laser and photoacoustic detector. In principle this latter technique might be able to detect down to the sub ppb level although the 1-30ppb level appears to be a more reasonable goal.<sup>8</sup> Limitations are primarily size, the need for a pure CO<sub>2</sub> source, and the requirement for critical optical geometries.

Chemiresistors have also been examined as sensitive surfaces for hydrazine detection.<sup>11</sup> Here a thin film whose conductivity changes upon exposure to hydrazine has been deposited across a series of interdigitized electrodes. Recent work with nickel dithiolene based chemiresistors has shown large responses to 200ppb hydrazine concentration and extrapolated detection limits in the sub-ppb range. However, these sensors have slow response times, requiring ~1-2 hours to reach equilibrium and hours (sometimes days) to reach pre-exposure signal levels.

A variation on the use of fiber optics is being performed in current work in which fiber

optics are used to develop a dosimeter for detecting hydrazine. <sup>12,13</sup> In this approach, a reagent that changes color on contact with hydrazine, phosphomolybdic acid, is entrapped in a sol-gel matrix on the outer surface of a silica fiber based sensor. Since the reaction is irreversible under atmospheric conditions, a dosimeter, rather than a real time monitor is evolving. The mechanism of detection is however through evanescent wave interaction, identical to the work described in this proposal. These results have also been analyzed in terms of developing a distributed fiber optic sensor network.

Reversible detection of hydrazines using FOCS incorporating immobilized triphenylmethane dyes, as demonstrated during the Phase I investigation, can avoid most of these above outlined limitations inherent with other strategies for reversible trace atmospheric hydrazine detection. Furthermore, FOCS based on triphenylmethane dyes possess a number of features which make them attractive for the real time monitoring of hydrazines. Previously discussed work<sup>1-3</sup> investigating the chemical bleaching of triphenylmethane dyes and subsequent restoration of color following removal of hydrazine has been shown to be rapid (~minutes). Furthermore, the use of evanescent wave based FOCS configurations allows for multiple reflections to probe the triphenylmethane dye at its interface with the fiber optic, thereby permitting high sensitivities to be realized.

When an exposed fiber optic is coated with a material whose interaction with the evanescent wave is modified upon hydrazine binding, a change in transmitted light through the fiber occurs, permitting hydrazine optical detection. When transmitted light through an optical waveguide strikes the interface between two transparent media, going from a medium of greater refractive index to one of lower refractive index, total internal reflection will occur when the angle of reflection  $\theta$  is larger than the optical angle  $\theta_c$ , as given by:<sup>14</sup>

$$\theta_c = \sin^{-1} n_2 / n_1 \tag{1}$$

In the above case, the evanescent wave will penetrate a distance  $(d_p)$  into the medium with a lower refractive index (i.e.  $n_2$ ). Although there will be no net flow of energy into the triphenylmethane dye, there will be an evanescent, nonpropagating field into the dye whose electric field amplitude E will be largest (i.e.  $E_o$ ) at the interfacial region decaying exponentially with distance Z from the surface. E will be given by:

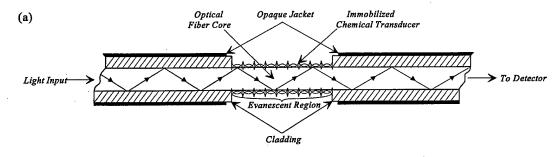
$$E = E_0 \cdot \exp(-Z/d_p)$$
 (2)

where  $d_p$  is defined as the distance required for the electric field amplitude to fall to exp(-1) of its value at the surface, as given by (Figure 2):

$$d_p = \frac{\lambda/n_1}{2\pi(\sin^2\theta - (n_2/n_1)^2)^{\frac{1}{2}}}$$
 (3)

Generally, penetration depth will depend on  $n_2$  and  $n_1$ , the wavelength  $\lambda$  and the angle of incidence. Since FOCS components can draw upon current optical communications technology, such sensors can be low cost, rugged and reliable.<sup>14</sup> Furthermore, triphenylmethane based FOCS can be utilized as part of a distributed sensor network unlike other hydrazines sensors discussed above.

In the optical sensor network being developed in this program the technique known as



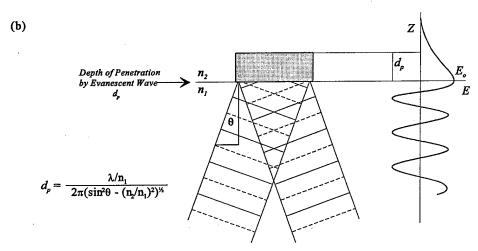


Figure 2. Schematic configuration for fiber optical detection (a) and generation of the evanescent wave at an interface between two optical media (b) used in this program for reversible detection of hydrazines.

Optical Time Domain Reflectometry (OTDR) will be used to probe immobilized triphenylmethane dyes on the fiber optic. Light entering the fiber will be reflected back towards the light source. A sensor site location within a fiber optic network can be identified by the time it takes for a pulsed signal to be reflected back to the source. Since light travels about 1 meter in 5ns with distance D being calculated by:

$$D = \frac{ct}{2n} \tag{4}$$

where c is the speed of light, t the round trip travel time of the input pulse, and n the core's average refractive index, the time the signal takes to return to the detector is directly related to the sensor site location.

As will become evident in this Final Report experimental work performed during Phase I resulted in clarifying the utility of the originally proposed distributed fiber optic sensor technology for the reversible detection of hydrazines based upon interaction with immobilized triphenylmethane dyes. Commercial application will result in the development of reliable fiber optic sensor technology for the continuous, reversible and simultaneous monitoring of hydrazines and other toxic vapors at distributed locations in the ppb concentration range.

# II. PHASE I TECHNICAL OBJECTIVES

The overall objective of this program was to demonstrate the feasibility of using selected triphenylmethane dyes immobilized onto optical fiber sensors as chemical transducers for the reversible detection of hydrazines. Scientific information obtained from this study was incorporated into a prototype hydrazine sensor built and tested during performance of this program. The utility of this fiber optic sensor technology for multisite OTDR detectors was also evaluated.

Technical objectives during Phase I were as follows:

- Immobilize triphenylmethane dyes onto the surface of fiber optics using thin-film thermal vacuum evaporation techniques.
- Perform detailed studies to determine the sensitivity that can be achieved from these selected triphenylmethane dyes for the reversible detection of hydrazines.
- Evaluate sensitivity, selectivity and response time that can be achieved by selected triphenylmethane dyes when coated onto the optical fiber sensor.
- Build and test prototype hydrazine sensors reflecting technology characterized during this program.

# III. WORK PERFORMED AND RESULTS OBTAINED

The Phase I experimental program was performed by completing the following two tasks:

- Task 1 Evaluation of Spectral Properties of Selected Triphenylmethane Dyes to Low Concentrations of Hydrazines
- Task 2 Performance Characterization of Immobilized Triphenylmethane Dyes on Fiber Optics for the Reversible Detection of Hydrazines

A summary of work performed in each task during Phase I and experimental findings follows.

# Task 1 Evaluation of Spectral Properties of Selected Triphenylmethane Dyes to Low Concentrations of Hydrazines

The objective of this task was to characterize spectral properties of selected triphenylmethane dyes initially deposited onto glass slides following their exposure to systematically varied hydrazine concentrations. Those triphenylmethane dyes showing a significant optical response together with signal reversibility were then incorporated into fiber optic sensors during performance of Task 2.

#### a. Experimental

Work in this task proceeded by initial fabrication of the experimental assembly schematically shown in Figure 3. This experimental arrangement, which was located in a fume hood, consisted of three components corresponding to respectively i) a capability for initially mixing the hydrazine containing sample and flowing it passed the sample of interest at a controlled rate, ii) an appropriately designed sample chamber for accommodating the glass slide under test, and iii) electrooptic components for initial generation of the probe beam and for its subsequent detection after interaction with the immobilized triphenylmethane dye on the glass slide surface.

The gas flow consisted of zero grade air which was introduced into the experimental arrangement through a rotameter into a Teflon gas mixing bag. As the gas mixing bag was filled with air, the required amount of hydrazine was introduced into the flow stream using a microliter syringe via a septum located before the gas mixing bag. After the mixing bag had been filled with the appropriate air/hydrazine mixture, the three way valve was switched to permit passage of the gas sample into the test chamber using a Teflon-lined bellows pump.

All tubing and connections exposed to the hydrazine containing air stream were fabricated from Teflon to prevent hydrazine decomposition. Exhaust from the bellows pump was scrubbed using a weak bleach solution. A schematic of the test chamber for accommodating glass slides incorporating immobilized triphenylmethane dyes is shown in Figure 4. The test chamber was machined from Teflon and contained appropriate connections for input and output of the hydrazine containing air stream. In addition, the experimental assembly contained two large ports for the incident probe beam and for subsequent detection of the output signal. The beam input port window was fabricated from a glass slide with one side covered with the triphenylmethane chemical transducer dye of interest. The light beam output port window consisted of an uncoated glass slide. Both glass slides were secured onto the chamber surface using O-rings to prevent leakage of hydrazine containing air into the atmosphere or of room air into the chamber. The photodetector was situated externally to the chamber next to the blank glass slide window as shown in Figure 4.

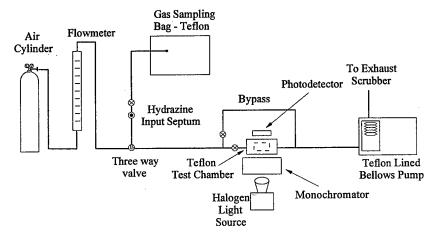


Figure 3. Schematic of experimental arrangement used during Phase I for initially screening the optical response of triphenylmethane dyes immobilized onto glass slides.

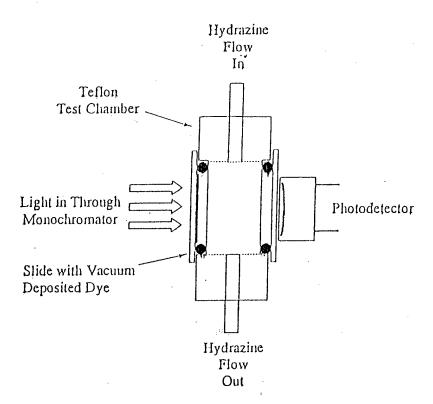


Figure 4. Schematic of test chamber incorporating glass slide containing immobilized triphenylmethane dye for hydrazine detection.

In this experimental configuration, electrooptic components consisted of a light source, monochromator, photodetector and electronic circuitry. The light source used initially was a halogen bulb. Illumination was passed through a grating monochromator (Oriel, Model-#77250) equipped with a grating (Oriel, Model # 77297) for use over the 200-700nm wavelength range. For dye-coated glass slides, light from the monochromator passed directly through this window and out to the photodetector as shown in Figure 4.

The output from a PIN photodetector (Sharp, 500 series) was fed into the amplification circuit shown in Figure 5. This circuit also possessed a zeroing amplifier which was later used in experiments performed on silica optical fibers during Task 2 at low hydrazine concentrations. The output from this circuit was sent to an analog-to-digital converter (Real time Devices, AD510) inside a computer. Data were captured using in house software.

#### b. Sample Preparation

Specific dyes deposited onto glass slides during this task were crystal violet (Baker Analyzed Reagent), Rosolic Acid (Aurin, Aldrich) Rhodamine B (Eastman) and Fluorescein (Aldrich). Triphenylmethane dye deposition onto glass slides was performed by thermal vacuum evaporation using an Edwards E306A Coatings System. Glass slides were obtained commercially (Fisher Scientific, Inc.) and cleaned thoroughly before use. Dyes were initially loaded into a partially covered molybdenum evaporation boat. After the substrate was positioned above the evaporation source, the chamber was pumped down to ~5 x 10<sup>-5</sup> Torr. Evaporation proceeded by heating the boat resistively. Typical applied powers were 500-600W. The dye was evaporated onto the substrate for 30s. Care was taken to ensure that the

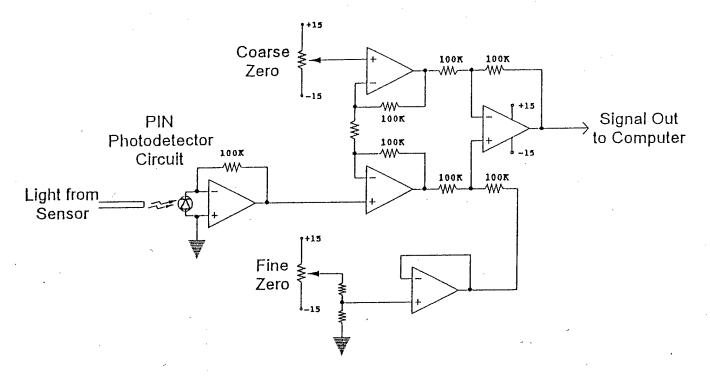


Figure 5. Circuitry used in conjunction with the PIN photodetector to detect signals from the chemical transducer dye when exposed to hydrazines.

distance between the substrate and the evaporation source was kept constant for each sample to ensure that films were of similar thickness. This procedure resulted in thin, uniform, partially transparent films of the triphenylmethane dye.

#### c. Experimental Results

Initial experiments were performed on glass slide substrates with optical signals being detected in the absorption mode. After coating, the sample was inserted into the sample chamber and the experiment performed using the flow system previously described.

The response of a glass slide coated with crystal violet towards air containing 100ppb hydrazine is shown in Figure 6. As can be observed, crystal violet responded reversibly to this hydrazine concentration. Some baseline drift was observed. The cause of this drift was not clear, but our previous experience has shown that there may have been some temperature dependence associated with the electrooptics. This particular experiment was performed at a wavelength of 600nm. Experiments were also performed at 500nm with similar results. Wavelengths of 600-800nm were preferable since laser diodes operating in this range are commercially available and inexpensive.

Experiments were also performed in a similar manner on the other three dyes. However, only minimal or no response was found towards 100ppb hydrazine over the wavelength range 500-700nm. When dye coated slides were exposed to greater amounts of hydrazine, color bleaching was observed. However with the experimental apparatus and electrooptics used here, no response to 100ppb was observed. Therefore, these dyes were not studied further and remaining experiments were performed on crystal violet or molecular variations of crystal violet.

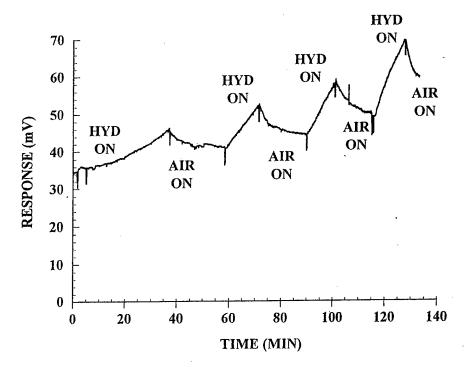


Figure 6. Response of a glass slide coated with crystal violet towards 100ppb hydrazine in air at 600nm.

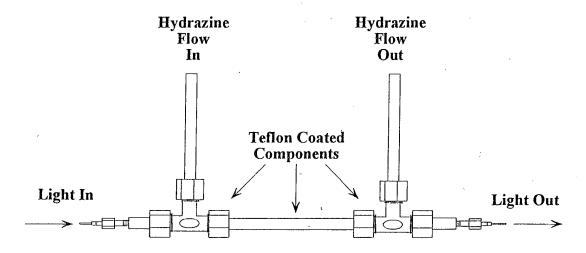
Completion of work in this task resulted in verifying that trace hydrazine could be reversibly optically detected by crystal violet dyes immobilized onto a glass slide. These experimental findings formed the basis of subsequent work addressed during performance of Task 2 in this Phase I program.

# Task 2 Performance Characterization of Immobilized Triphenylmethane Dyes on Fiber Optics for the Reversible Detection of Hydrazines

## a. Optical Response to Hydrazine, 1,1'-Dimethylhydrazine and Monomethylhydrazine

The objective of work performed in this task was to incorporate onto silica fiber optic sensors those dyes which had demonstrated sensitivity and reversibility to the subject hydrazine vapors during Task 1. These sensors were operated in both evanescent wave and absorption configurations with initial dye deposition proceeding using previously discussed thermal vacuum techniques.

Silica fiber optic sensors operating in the evanescent wave mode were incorporated into the test chamber shown schematically in Figure 7. A Teflon tube was used to provide an air tight seal, mechanical rigidity, and to prevent hydrazine decomposition. The optical fiber was inserted into and removed from the chamber tube through plastic septa held in Teflon tee joints. The third arm of these connections served as input or output for the hydrazine containing air stream. The optical fiber sensor was connected directly to the monochromator and photodetector using SMA connectors external to the chamber. Electrooptical components were initially the same as used during Task 1. Later however the original illumination source, a halogen lamp with a grating monochromator, was replaced with a commercially



Fiber Optic Test Chamber

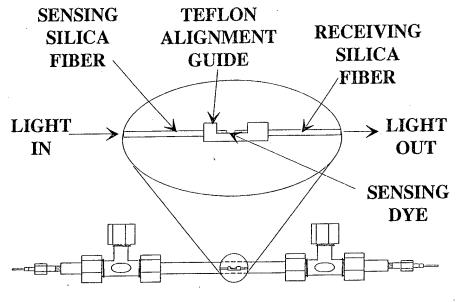
Figure 7. Schematic of sample chamber used for hydrazine detection in silica fiber optic sensors operating in the evanescent wave mode.

available laser diode operating at 635nm possessing a maximum power output of 3mW (Model SPMT 03-635-3, Power Technology, Inc.).

In addition to these light sources, a light emitting diode (LED) operating at 660nm and 2000mcd (Archer) was also evaluated for this application. Although optical signals could be detected with this source, they were much less intense than the laser diode and therefore a decision was made to place emphasis on electrooptical measurements using the 635nm laser diode as the illumination source. We anticipate that with a more sensitive detection system, it may however be possible to use an LED in the future. The advantage of an LED is that it would be significantly less expensive than a laser diode. However, selection of the probe beam source and detection system for commercial sensors will depend on the sensitivity required in the final device, and costs associated with both the optical source and detection system.

Measurements were also performed in which the fiber optic signal detection mode was changed from an evanescent wave mode to the absorption mode. This change was made in part to address the effect of humidity. Water absorption onto the distal end of the fiber was not expected to change absorption intensity. To perform this measurement, the fiber sample chamber in the experimental apparatus was changed to the configuration shown in Figure 8. Crystal violet was coated by thermal vacuum evaporation, as described previously, onto the distal end of a silica fiber optic sensor. The experimental apparatus was modified to ensure that the sensing and receiving fiber were aligned. Upon exposure of this sensor to 10ppm hydrazine in air, a response of ~3mV was observed as shown in Figure 9. This compared to a response of ~0.5mV observed at this stage of our investigation for the same hydrazine concentration when detected by crystal violet in the evanescent wave mode. Hydrazine in air at 1ppm was also clearly detected in the absorption mode as shown in Figure 10.

To detect hydrazine concentrations <1ppm, a new experimental arrangement was fabricated as schematically shown in Figure 11. In this arrangement, hydrazine was supplied



TEST CHAMBER

Figure 8. Schematic of experimental arrangement used to detect hydrazine in the absorption mode by coating the sensing dye on the distal end of the silica fiber optic.

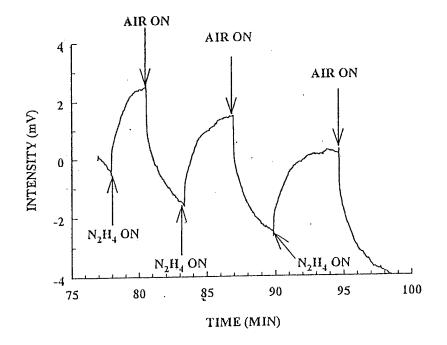


Figure 9. Response towards 10ppm hydrazine in air in the absorption mode of the silica fiber optic with its distal end coated with crystal violet.

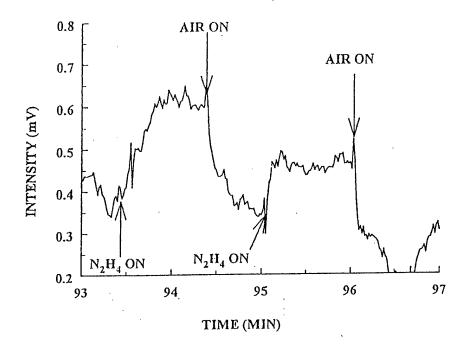


Figure 10. Response towards 1ppm hydrazine in air in the absorption mode of a silica fiber optic with its distal end coated with crystal violet.

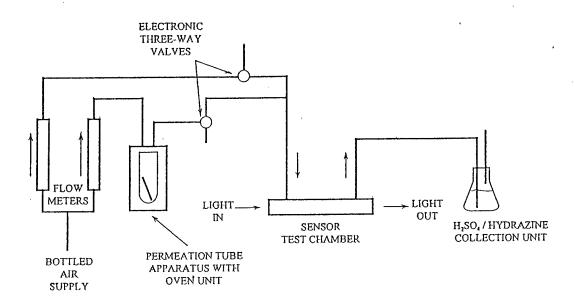


Figure 11. Schematic of revised experimental fiber optic sensor configuration used to detect hydrazine in air at concentrations <1ppm.

through a commercially available permeation tube (Kin-Tek Laboratories, HRT). By adjusting temperatures, the hydrazine permeation rate was varied from 10-100ng/min. Air flow rates over the permeation tube were also varied to achieve concentrations over the range 10-1000ppb in air. Quantitative determination of hydrazine in the air stream being passed over the fiber optic sensor was performed by introducing the effluent stream into a 0.1M  $H_2SO_4$  trap. The hydrazine concentration in acid was then determined using a commercially available ASTM colorimeter test kit (Hach, Hydraver 2). With known exposure time and flow rate, the average exposure level of the fiber optic sensor towards hydrazine could then be determined.

Our initial experiments using this revised experimental configuration emphasized crystal violet as the chemical transducer for hydrazine detection. However, no response in the evanescent wave mode at concentrations <1ppm were initially observed. We speculated that the reason was that the wavelength of maximum intensity ( $\lambda_{max}$ ) for crystal violet was 590nm<sup>13</sup> while the laser diode wavelength used in these experiments was 635nm. To obtain greater sensitivity required that  $\lambda_{max}$  for the triphenylmethane more closely overlap the emitting wavelength of the laser diode light source. To address this issue the closely related triphenylmethane dye malachite green, possessing a  $\lambda_{max}$  of 621nm, <sup>15</sup> closer to that of the laser diode, was employed. Molecular structures for crystal violet and malachite green are compared in Figure 12.

The carbinol analog of malachite green, malachite green carbinol hydrochloride (Aldrich Chemical Co.) was converted to the chloride salt of malachite green by dissolving the corresponding carbinol hydrochloride in water, as shown in the reaction scheme by Figure 13. The chloride salt was isolated by evaporating the aqueous solution. Fiber optic sensors were then prepared by thermally vacuum evaporating the dye onto the optical fiber surface. The

CRYSTAL VIOLET:  $X = N(CII_3)_2$ MALACHITE GREEN; X = H

Figure 12. Comparative molecular structures of crystal violet and malachite green.

Figure 13. Reaction scheme used during Phase I to convert malachite green carbinol hydrochloride into malachite green chloride.

response of the fiber optic sensor based on malachite green in the evanescent wave mode is shown in Figure 14. As can be observed, concentrations over the range 10-35ppb hydrazine in air were reversibly detectable. This result indicated that using dyes with a  $\lambda_{\rm max}$  closer to the light source could provide significantly enhanced sensitivity towards the optical detection of trace hydrazines.

In addition to hydrazine, we also examined the response of fiber optic sensors to 1,1'-dimethylhydrazine (UDMH) and monomethylhydrazine (MMH) in the evanescent wave mode. The experimental apparatus used was that described previously using a laser diode at 635nm as the light source. Permeation tubes (KinTek Laboratories) served as UDMH or MMH sources. Hydrazine detection was based upon immobilized malachite green. Figures 15 and 16 show the response of the sensor to 1ppm and 50ppb, of UDMH in air. As can be observed, these fiber optic sensors exhibited a clear reversible response to UDMH. Figure 17 shows the response of the sensor to 81ppb MMH. Again a clear reversible response was observed.

Initial experiments were also performed in order to test sensor stability. A sensor based on crystal violet was fabricated and tested three days after preparation. The response of this sensor towards 40ppm hydrazine is shown in Figure 18. The same sensor was retested with 40ppm hydrazine the following day (four days after preparation) as shown in Figure 19. As can be observed, the response was stable. Figure 20 shows the response of the same sensor towards 40ppm hydrazine after an additional two days of testing (six days after preparation) where a smaller response was observed. The reason for this smaller signal may have been a consequence of the relatively thick triphenylmethane dye deposited onto the fiber optic substrate where reversible mediation of hydrazine to and from the fiber optic/dye interfacial region became progressively more difficult at higher hydrazine concentrations. We anticipate that such limitations would be circumvented by direct chemical bonding of a dye monolayer onto the silica fiber substrate. This issue will be addressed in detail during

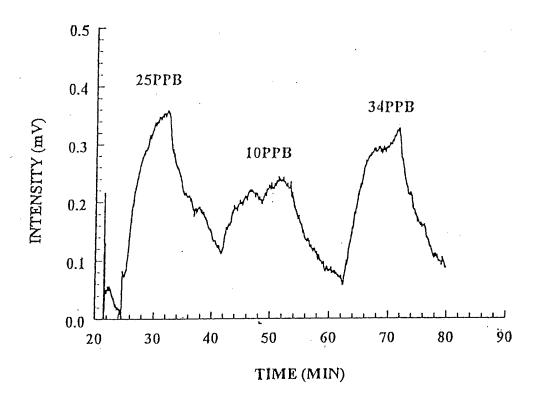


Figure 14. Response towards 10-35ppb hydrazine in air of a sensor based on malachite green in the evanescent wave mode.

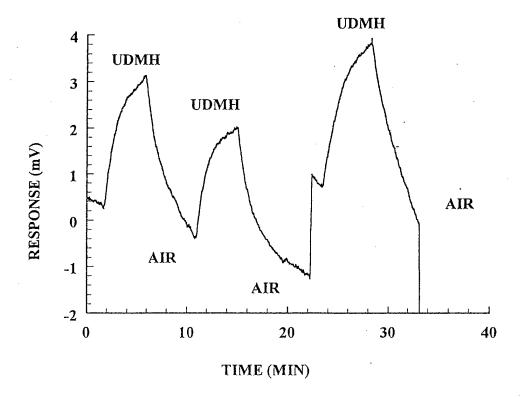


Figure 15. Response of a malachite green based fiber optic sensor to 1ppm UDMH in air operating in the evanescent wave mode. The light source was a laser diode operating at 635nm.

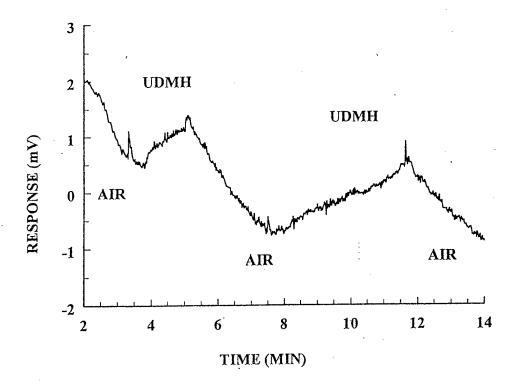


Figure 16. Response of a malachite green based sensor to 50ppb UDMH in air operating in the evanescent wave mode. The light source was a laser diode operating at 635nm.

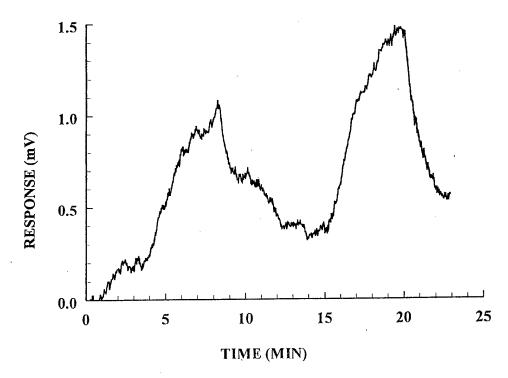


Figure 17. Response of a malachite green based sensor to 81ppb MMH in air operating at the evanescent wave mode. The light source was a laser diode operating at 635nm.

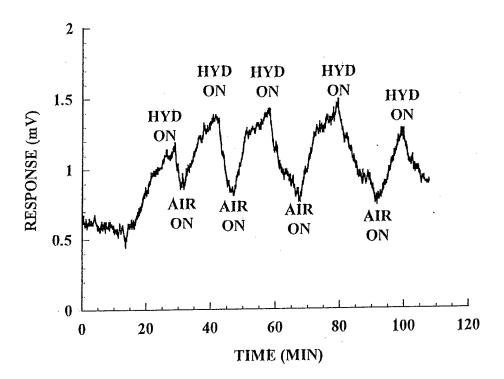


Figure 18. Response towards 40ppm hydrazine of a sensor prepared by evaporation of crystal violet onto a silica optical fiber. This test was performed three days after preparation.

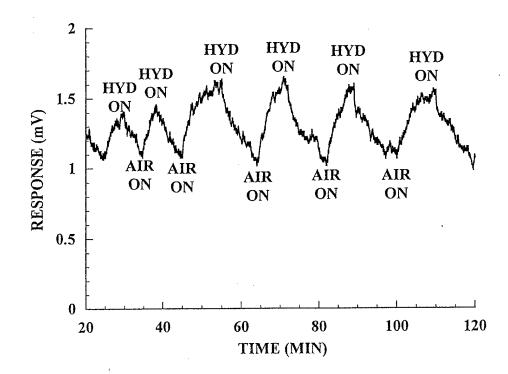


Figure 19. Response towards 40ppm hydrazine of sensor used in Figure 18 after four days of testing.

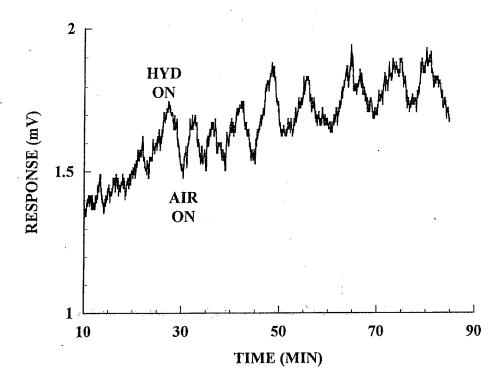


Figure 20. Response towards 40ppm hydrazine of sensor shown in Figure 19 after six days of testing.

performance of Phase II. Furthermore it should be noted that these latter measurements were performed using hydrazine concentrations significantly higher than anticipated in the field. Fiber optic sensors using immobilized triphenylmethane dyes prepared during Phase I exposed to ~10ppb hydrazine would of course be expected to exhibit significantly longer lifetimes.

Completion of work in this section clearly showed that application of triphenylmethane dyes possessing absorption close to the laser diode source were capable of reversibly detecting trace atmospheric hydrazine down to concentrations of 10ppb when immobilized on a silica fiber optic substrate. Sensors were also demonstrated as reversible to 1,1'-dimethylhydrazine and monomethylhydrazine.

#### b. Evaluating Ammonia as a Potential Interferant for Hydrazine Detection

The experimental apparatus used to detect the effect of ammonia on fiber optic sensor performance was based on that described previously in Task 1 (Figure 3). A Teflon sampling bag was filled with air and the desired quantity of ammonia injected into the bag using an air-tight syringe. This gas mixture was then pumped past the fiber optic sensor using a bellows pump. The optical fiber sensor chamber and electrooptics were those used previously. The light source was again a 635nm laser diode.

Figure 21 shows the typical response of a malachite green based sensor towards 20ppb hydrazine in air. In comparison, the fiber optic sensor response towards 1ppm ammonia is shown in Figure 22. This response towards 20ppb hydrazine was  $\sim 0.4$ mV or 0.02mV/ppb. For ammonia in air, the response was  $\sim 0.5$ mV towards 1ppm, or  $5 \times 10^4$ mV/ppb. This

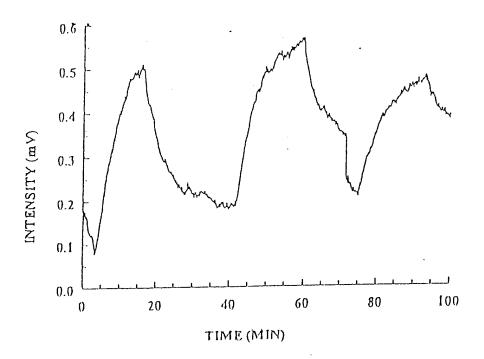


Figure 21. Response of a malachite green based fiber optic sensor operating in the evanescent wave mode towards  $20ppb\ N_2H_4$  in air.

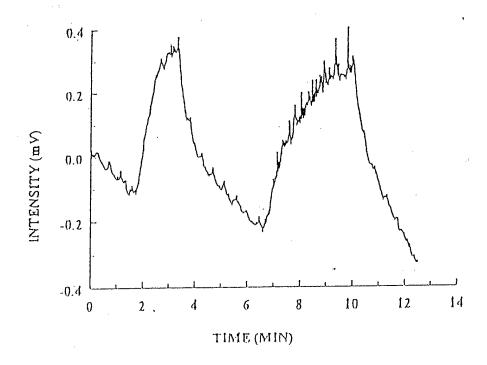


Figure 22. Response of a malachite green based fiber optic sensor operating in the evanescent wave mode towards 1ppm NH<sub>3</sub> in air.

indicated that the unoptimized fiber optic sensor based on malachite green was approximately forty times more sensitive to hydrazine than towards ammonia. Figures 23 and 24 show the response of the sensor towards 100ppb and 50ppb of ammonia in air, respectively. As can be observed, there was only a very weak response observed for 50ppb ammonia in air.

To further study the effect of ammonia on the fiber optic sensor, we examined the wavelength dependence response towards both ammonia and hydrazine in air in the evanescent wave mode. The light source was changed from the laser diode to the halogen bulb and grating monochromator. The intensity of the sensor response to either ammonia or hydrazine in air was recorded and plotted relative to the sensor response in air alone. Figure 25 shows results obtained when the fiber optic sensor was exposed to 500ppb hydrazine and 10ppm ammonia in air. This figure shows a large difference in wavelength response dependence towards these two species. Specifically, there was a large response to ammonia at ~520nm while only a weak response to hydrazine. Conversely, at wavelengths greater than 630nm, the response to hydrazine increased while that for ammonia decreased. Note that at 650nm, the sensor was approximately forty times more sensitive to hydrazine than to ammonia. This was similar to that previously observed.

Figure 25 also shows that at wavelengths above 650nm, the difference in sensor response towards these two species becomes even greater. We therefore examined the fiber optic

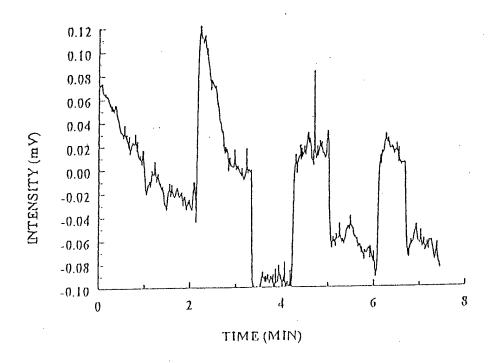


Figure 23. Response of a malachite green based fiber optic sensor operating in the evanescent wave mode towards 100ppb NH<sub>3</sub> in air.

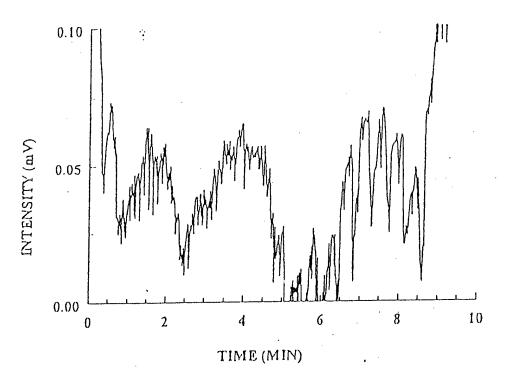


Figure 24. Response of a malachite green based fiber optic sensor operating in the evanescent wave mode towards 50ppm NH<sub>3</sub> in air.

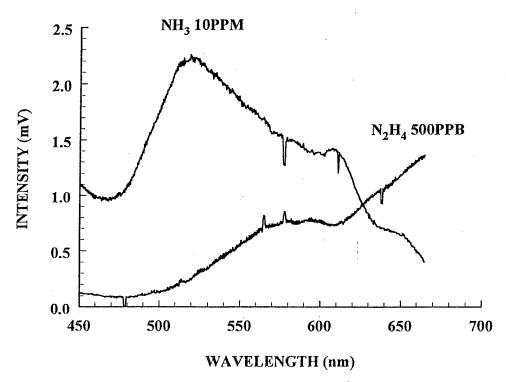


Figure 25. Wavelength response dependence of a malachite green based fiber optic sensor operating in the evanescent wave mode towards 500ppb  $N_2H_4$  and 10ppb  $NH_3$  in air. Intensities are relative to the sensor in air.

sensor spectra when exposed to 500ppb hydrazine and 10ppm ammonia over the wavelength region 600-1100nm. This was performed using the experimental arrangement shown in Figure 11 but substituting a different monochromator grating in order to achieve higher wavelengths. Figure 26 shows results obtained. Again, spectra obtained were relative to the fiber optic sensor exposed to air. This plot shows maximum sensitivity to hydrazine occurring at ~720nm. However, ammonia response was also at a maximum in this region, although opposite to that for hydrazine. This result indicates that this wavelength would not be suitable for the subject fiber optic sensor since the response to hydrazine would be negated due to the opposite response for ammonia. A more appropriate wavelength for hydrazine detection would be in the region 680-700nm where the response to ammonia was at a minimum. In Figure 25, the wavelength where response towards both 500ppb hydrazine and 10ppm ammonia are equal occurs at ~625nm while this point occurs at ~680nm in Figure 26. This shift may be due to the experimental apparatus in which two different monochromator gratings were used, rather than to differences in the fiber optic sensor itself.

In addition to the wavelength dependence of the sensor response towards both hydrazine and ammonia, we also examined the wavelength response dependency to MMH and UDMH. Figure 27 shows a comparison of results using a malachite green based optical fiber towards respectively hydrazine, ammonia, MMH and UDMH. Differences in optical response between these hydrazines was probably a consequence of differing basicities. These results suggest that the maximum differential between responses to ammonia and UDMH will occur further into the infrared, ~850 or ~980nm. These wavelengths are readily accessible with inexpensive and commercially available light sources. By appropriate manipulation of

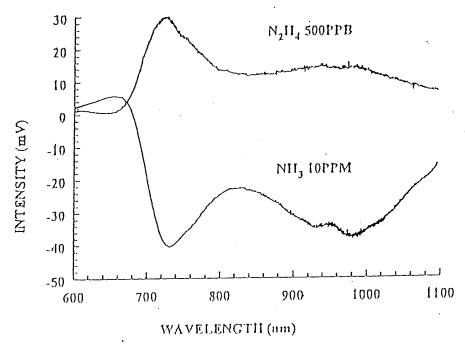


Figure 26. Wavelength response dependence of a malachite green based fiber optic sensor operating in the evanescent wave mode towards  $500ppb\ N_2H_4$  and  $10ppm\ NH_3$  in air. Intensities are relative to the fiber optic sensor in air.

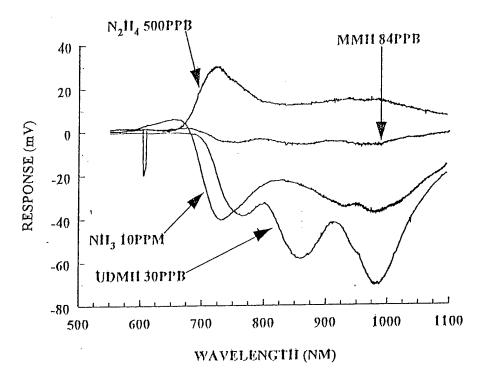


Figure 27. Wavelength dependence of the response of a malachite green fiber optic sensor operating in the evanescent wave mode towards 500ppb  $N_2H_4$ , 10ppm  $NH_3$ , 84ppb MMH and 30ppb UDMH. Intensities are relative to the fiber optic sensor in air.

immobilized triphenylmethane dye chemistry and probing the sensing region with longer wavelengths, discrimination between hydrazines and ammonia >1000 are expected to be reasonably achievable.

#### c. Evaluating Water as a Potential Interferant for Hydrazine Detection

The influence of humidity upon fiber optic sensor response was addressed using the general experimental arrangement shown previously in Figure 3 where humidity was introduced into atmospheric samples by injecting water into a Teflon gas sampling bag. The fiber optic sensor was based on crystal violet operating in the evanescent wave mode. Again, a laser diode operating at 635nm was used as the light source.

Initial experiments were performed by exposing the fiber optic sensor to 3000ppm water vapor in air in the absence of hydrazine. The response observed is shown in Figure 28. As can be observed, there was a clear response to water. The response was very rapid and in the opposite direction to that found for hydrazine.

Since the water response was both very rapid and opposite of that for hydrazine, it seemed likely that this was not due to interaction of humidity with the transducer dye, but humidity absorption onto the fiber surface. This supposition was tested by placing an uncoated fiber into the test apparatus and exposing it to water vapor as in the previous experiment. Results of this experiment are shown in Figure 29 which indicated that the fiber optic surface rather than the triphenylmethane dye was responsible for the optical response.

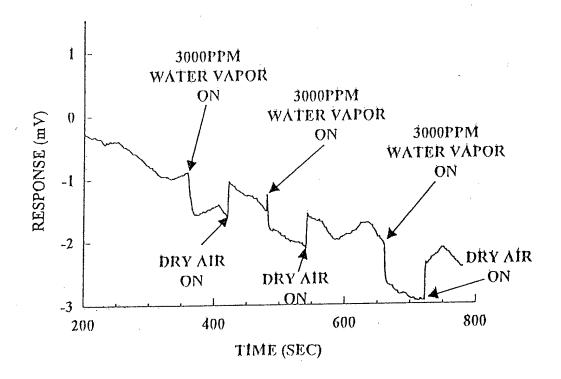


Figure 28. Response of a crystal-violet-coated silica optical fiber to 3000ppm water vapor in air at 635nm in the evanescent wave mode.

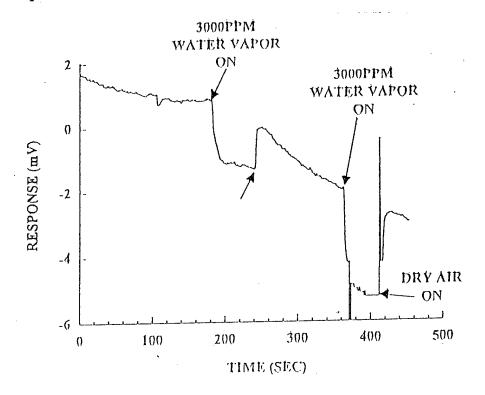


Figure 29. Response of an uncoated silica optical fiber to 3000ppm water vapor in air at 635nm in the evanescent wave mode.

This suggested that more homogeneous triphenylmethane dye coatings on the fiber optic surface would minimize or eliminate humidity related signals.

#### d. Towards Distributed Fiber Optic Sensor Measurements

Preliminary work was performed to verify the utility of candidate electrooptical components to be utilized in a distributed fiber optic sensor network. As we have previously discussed, to realize such a network requires high speed components so that spatial resolution between individual sensing sites can be obtained. This spacial resolution will be a function of the minimum light pulse width and frequency cutoff for the detector. Preliminary work towards implementing this network proceeded using standard commercially available components. The fiber optic illumination source used was a SPMT(633-5) laser diode. This source had a pulsewidth of 25ns which permitted a spatial resolution of 7.5m. The detector used for this source was a SFH250 (Siemens) PIN photodiode. The experimental arrangement, including the source pulsing and detector circuitry is shown in Figure 30. A Tektronix 2213 oscilloscope was used to collect data from the detector. An experiment was performed in which the light pulse was delayed by use of a 60m fiber optic cable to simulate a distance. In practice, the light pulse was launched from the laser diode and then detected after propagation through this delay line. Figure 31 shows the results of this experiment. The top trace shows the generated optical pulse and the bottom trace the detected signal. A clear time delay of ~200ns, due to light pulse transmission time through the fiber optic cable, was observed. This experiment verified, using readily commercially available components, that spatial resolution between individual hydrazine sensor sites separated by tens of meters could be achieved.

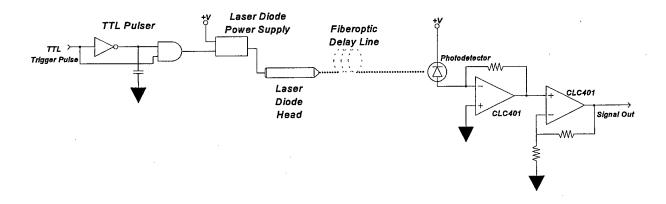


Figure 30. Experimental arrangement showing laser diode pulsing and detector circuitry for detecting narrow light pulses required to obtain spatial resolution in a distributed fiber optic network for determining atmospheric hydrazine concentrations.

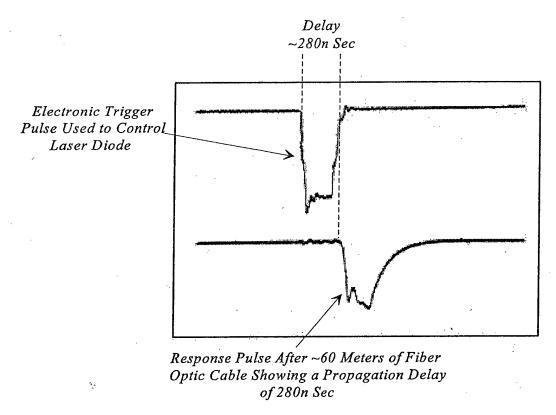


Figure 31. Oscilloscope traces showing detection of delayed light pulse which corresponds to spatial resolution of ~7.5m.

### IV. SUMMARY OF PHASE I RESULTS

- Hydrazine and its congeners, UDMH and MMH, were reversibly detected at concentrations levels down to 10ppb in air using triphenylmethane dyes immobilized onto the surface of silica fiber optic sensors operating in the evanescent wave mode.
- Highest sensitivity was found using malachite green as a triphenylmethane dye immobilized onto the fiber optic substrate. This dye possessed a  $\lambda_{max}$  of 621nm, close to that of the laser diode probe beam employed.
- Unoptimized fiber optic sensors studied to date have a sensitivity towards ammonia, a potential interferant, approximately forty times less than for hydrazine. Significant differences were found in the wavelength dependence response for malachite green fiber optic sensors operating in the evanescent wave mode towards hydrazine, ammonia, MMH and UDMH. As a consequence by appropriate manipulation of immobilized triphenylmethane dye chemistry and probing the sensing region with longer wavelengths, discrimination between hydrazines and ammonia >1000 would be a reasonably achievable goal.
- Fiber optic sensors also exhibited some sensitivity towards atmospheric humidity. Analysis of results however showed that such responses were due to water adsorption onto the fiber optic surface rather than interaction with the triphenylmethane dye. This indicates that more homogeneous triphenylmethane dye coating strategies to be adopted during Phase II will eliminate or minimize such effects.

- Initial experiments were performed which showed that a spatial resolution for fiber optic sensor locations of several tens of meters can easily be obtained. This indicates that a distributed network for the reversible detection of trace hydrazines can be fabricated using standard electrooptical components.
- Ensuring commercial success for distributed fiber optic sensor technology to emerge as a consequence of Phase I and II efforts depends in part on previous experience relating to fiber optic sensor product development, manufacturing and marketing. Towards this end Eltron is currently working towards commercial development of a multisite toxic gas detector system utilizing fiber optic signal transmission. We consider this to be our "first generation" fiber optic signal distributed sensor technology which will be commercialized during performance of the Phase II program and will ensure rapid market entry for optimized "second generation" distributed fiber optic sensor technology operating in the evanescent mode to emerge towards the conclusion of the Phase II program.

#### V. ESTIMATE OF TECHNICAL FEASIBILITY

#### A. Background

The overall objective of this program was to demonstrate the feasibility of using selected triphenylmethane dyes immobilized onto optical fiber sensors as chemical transducers for the reversible detection of hydrazines. Scientific information obtained from this study was incorporated into a light weight prototype hydrazine sensor built and tested during performance of this program. The utility of this fiber optic sensor technology for multisite OTDR detectors was also evaluated.

A viable instrument for the distributed detection of trace hydrazines with a fiber optic sensor network requires two major components: the chemical transducer and the electrooptics. The most critical of the two is the chemical transducer. Requirements for a useful transducer include: adequate sensitivity upon interaction with trace hydrazines; adequate response times; reversibility; long-term stability; and selectivity towards hydrazines over potential interferants. Sensitivity is defined by the proposed American Congress of Government Industrial Hygienists (ACGIH) regulations concerning permissible exposure limits. The definition of adequate long-term stability will depend on the cost and difficulty of sensor replacement. We anticipate for this application, stability of several months should be acceptable. A response time of several minutes is expected to be acceptable in this application. Definitions for acceptable selectivity over potential interferants also depends upon the specific application.

The results obtained during Phase I indicate that triphenylmethane dyes selected as potential chemical transducers meet these requirements. First, hydrazine, UDMH and MMH were all detected at levels of 10-100ppb, as shown in Figures 14, 16 and 17, respectively. This level of detection will be required to meet the proposed ACGIH regulations concerning permissible exposure limits and therefore the technical approach proves acceptable.

A response time of several minutes was also obtained for the sensors prepared and studied here (Figures 9 and 10). Since these figures show both the response times of the

sensor and the time required for the hydrazine to pass through the flow system and into the sample chamber, true sensor response times are probably somewhat less than observed. Additionally, sensors prepared with a thinner transducer dye layer are expected to exhibit faster response times. Thinner layers can be achieved by covalent binding of the dye molecule to the fiber surface as discussed below. Based on these results, we believe that response times of three to four minutes will be achieved and found acceptable for this application.

Sensor reversibility was also evident from experimental work performed during this program. For example, Figure 19 shows the response of a crystal violet coated optical fiber to 40ppm hydrazine in air. Reversibility can be judged by the return of the signal to the base line, as observed in Figure 19. If the sensor was not completely reversible, then the signal would not return to the baseline. In some of our data there was evidence for baseline drift. We believe that this was due to temperature dependence by the electrooptics. Any commercial device will need to include some mechanism for temperature compensation of the electrooptics. This can be achieved through the use of an internal reference beam.

Initial experiments to test the stability of the sensor indicated a lifetime of several days (Figures 18-20). This may not be acceptable for the desired instrument. To enhance stability, two aspects of the chemical transducer can be modified. The first is to modify the binding strength of the dye molecule with the hydrazine. The interaction between the hydrazine molecules and the transducer dye is an electron transfer from the former to the latter which leads to bond formation between the hydrazine and the central carbon atom of the dye molecule (Figure 1).<sup>1-3</sup> By increasing the electron density at the central carbon atom, this interaction can be weakened leading to enhanced stability. Modification of the electron density can be achieved by substitution of electron donating groups on the dye phenyl rings. Potential substituents include alkyl and amine groups.

A second aspect of sensor stability relates to the environment in which it is operating. It will be necessary to ensure that the transducer dye molecule will remain on the fiber surface and will not be susceptible to either mechanical impact or dissolution in the condensation known to occur at deployment sites. To prevent the latter from occurring, covalent binding of the transducer dye molecules to the silica fiber surface will be necessary. This will be achieved through the use of silica coupling agents.

Mechanical impact can be reduced through the use of an outer protective layer at the sensor region. The problem is how to protect the sensor while still permitting the hydrazine vapor to reach the surface. Because hydrazines of interest here are so reactive, the protective layer needs to be inert. One potential layer is a porous membrane fabricated directly on the fiber surface. Teflon and other fluorinated polymers are potential membrane materials. This approach would be the most desirable because it is essentially a simple coating on the sensor itself and would therefore be easy to fabricate. If this membrane layer proves to be unacceptable because it prevents diffusion of the hydrazine to the sensor surface or otherwise interferes with the detection mechanism, a mechanical baffle-type device would then be used to protect the sensor surface. This approach is less desirable as it adds another component to the device and would increase manufacturing costs as well as require a slightly larger space for the sensor. However, these two disadvantages are not expected to prevent deployment.

The final issue for determining the technical feasibility of this approach for hydrazine detection is one of interferants. For detection of hydrazines at the Cape Canaveral site, the major interferants will be ammonia and water. Work during Phase I showed that sensors responded to both of these species. The response of the sensor to ammonia was approximately 40 times less than towards hydrazine. The experimental results (Figures 25 and 26) showed that further discrimination should be achievable by the appropriate choice of wavelength or by probing the sensor with two wavelengths. We estimate that a determination factor of 1000 should be achievable by either of these routes.

The effect of water as an interferant on the fiber optic sensor is shown in Figure 28 where a response can be observed. However, a response of the same magnitude was also observed for an uncoated fiber (Figure 29). Additionally, response time towards water was identical in both of these cases but much less than observed towards hydrazine. These results indicated that the response to water vapor was not due to interaction with the dye, but simple water adsorption onto the fiber optic surface. This indicates that the sensor response to water can then be reduced by preparing the sensors so that there is little or no exposed blank fiber. Covalent binding of the transducer dye to the silica fiber optic surface will aid in obtaining a more uniform and less porous surface and is expected to reduce the sensor response to water.

The second component of the fiber optic sensing instrument relates to electrooptics used. All work performed during this Phase I program used commercially available equipment. For a single site monitor, a LED can serve as the light source with a PIN photodiode as the detector. We estimate that overall costs of electrooptic components would be in the \$10-20 range for a single site which is expected to be acceptable from the viewpoint of manufacturability and marketing.

In addition to the single site sensor, results from Phase I also point to the feasibility of a distributed fiber optic sensor network. For example, Figure 31 shows that using standard electrooptic components, spatial resolutions of ~7.5m were easily achievable. Enhanced electrooptics will allow for even higher spatial resolutions.

Although the specific parameters for a distributed fiber optic hydrazine sensor network are not known at this point, we can show the feasibility of such a network, in terms of electrooptics requirements, by making some assumptions about the network.

Three issues for defining the fiber optic sensor network will be considered 1) fiber optic sensor network architecture, 2) power budget and number of sensor sites, and 3) spatial resolution between sensor sites. Although each of these issues are interrelated each will be individually discussed.

# **B.** Fiber Optic Sensor Network Architecture

To access individual sensor sites within a fiber optic network will require some form of multiplexing. Since the fiber optic sensor network for detection of trace hydrazines will require spatial resolutions no less than several meters, time division multiplexing will be the most convenient to implement and still provide the required degree of spatial resolution. Several types of network architectures can be implemented in a multisite fiber optic sensor network based on time division multiplexing. From experimental results obtained in this program the linear array network (Figure 32) would appear to be the best alternative. The optical signal will be forced to reflect back immediately after interaction with each hydrazine

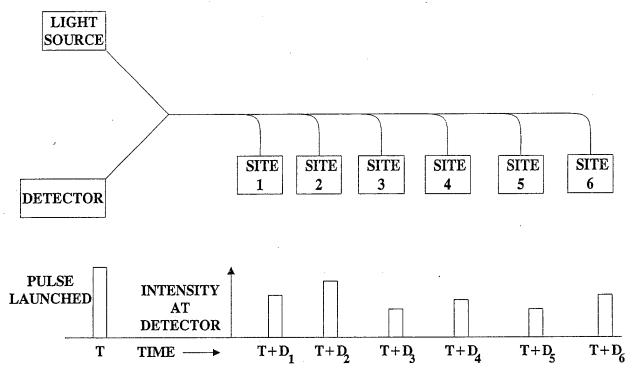


Figure 32. Six site linear array network for use with back reflected fiber optic geometries showing the time sequence converting the spatial domain to the time domain.

fiber optical sensor via a mirror applied to the distal end resulting in a second pass through the sensor region and back to the instrument. Figure 32 also illustrates how spatial information in the network becomes converted into the time domain using this type of multiplexing.

# C. Power Budget and Number of Sites for Detection

The second issue in designing the fiber optic sensor network is the power budget. The light intensity put into the system, the dynamic range of each individual sensor and losses through the system define the power budget and determine the maximum number of sites that can be incorporated within the sensor network. A detailed and specific power budget for a fiber optic sensor network cannot be performed at this stage due to the lack of data. However, a general network can be designed to show that a distributed network can be implemented with technology to be developed during Phase II.

Figure 33 shows a schematic six site model network based on a linear array with coupling ratios as shown. These ratios are chosen to ensure that equal amounts of light reach each fiber optic sensor. For a general sensor network design, it will be assumed that a dynamic range of 20dB (1%,  $\pm 0.2$ ppm) will be sufficient. Additionally, we assume a base detection limit of 10nW (-50dBm) for the sensor to ensure that detection is well above the noise limit. These two parameters then require a light input of  $1.0\mu$ W into each sensor. For a six sensor network, total input power required would be  $6.0\mu$ W. For a twelve sensor network,  $12.0\mu$ W would be required.

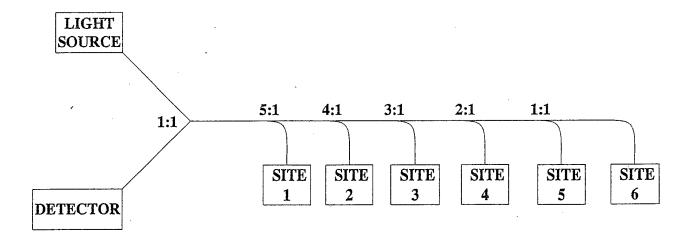


Figure 33. Six site linear array network showing the required coupling ratios each ensuring that equal light intensities reach each site.

The next step in this analysis is to account for losses due to optical couplers, splices and fibers. Assuming a total light path of 0.5Km and a loss of 10dB/Km in the  $200\mu m$  fiber, and a 1.0dB insertion loss per coupler, this increases the input power required in a six site network to  $120\mu W$ . For a 12 site network with a 1km path length and identical coupler losses, input power required is 3mW. To put these power requirements into perspective, the laser diode used during Phase I had a light output of 3mW continuous duty. For the fiber optic sensor network, the light source must be pulsed at a very small duty cycle, hence light output can be easily increased by a factor of five or ten for the same diode using higher current pulses at small duty factors. Thus this laser diode output is still more than adequate, if used at small duty factors, to provide the power necessary to implement a 12 site network. Although approximate, these calculations do show that a 12 site network, based on sensing elements identified during this program are reasonable.

### D. Spatial Resolution

The final issue in defining the fiber optic sensor network to be adopted during commercial development of this technology relates to the spatial resolution that can be achieved between individual sensing sites. Since the network will operate by time division multiplexing, the minimum spatial resolution achievable will be defined by the minimum width of the light pulse emitted, dispersion effects in the optical fiber cable and the maximum frequency at which the detector operates. To achieve a spatial resolution of 2m requires a modulation frequency of 150MHz (equivalent to a pulse width of 3.5ns) and a detector cutoff frequency of at least 150MHz. The latter parameter will be readily obtained using commercially available components. However, the short pulse width is more difficult. For example, the laser diode used in this program had a pulsewidth of 25ns equivalent to a spatial resolution of 7.5m. To obtain spatial resolution between sites of 2m with this particular laser diode will require artificially increasing the distance between sites by simply adding a coil of fiber. This is illustrated in Figure 34.

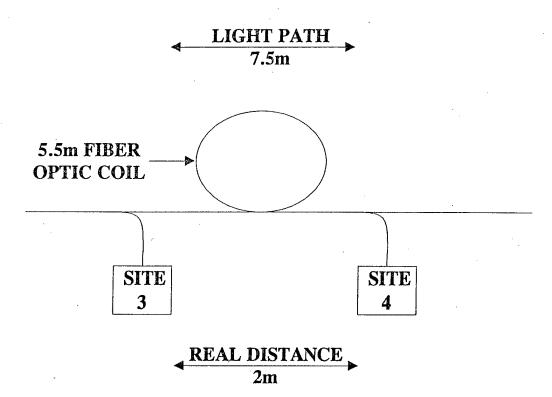


Figure 34. Schematic illustration showing the use of a fiber optic coil as one possible option for increasing the light path to achieve a narrower site spatial resolution.

# VI. RELATIONSHIP WITH FUTURE RESEARCH OR R&D EFFORTS

Successful completion of this overall three phase program will result in development of a distributed multisite fiber optic chemical sensor for real time monitoring of trace hydrazines in the atmosphere.

Anticipated results of the proposed program will be:

- To clearly identify parametric variables influencing the utility of the subject fiber optic chemical sensor instrumentation for detection of hydrazines.
- To optimize individual components of the overall monitoring network. This includes chemical, electrooptic and software components.
- To design a component instrumentation system compatible for deployment on site.
- To confirm the utility of this instrumentation technology under representative conditions.

We anticipate that mature instrumentation technology will find a variety of applications for both single-site and perimeter monitoring of hazardous chemicals. Phase II work will provide the necessary experience for fabrication and performance verification of advanced preproduction prototype instrumentation for achieving the detection of hydrazines in both a single-site mode and as a perimeter monitor via a distributed network. As a consequence, this will provide a foundation for subsequent commercialization during Phase III.

## Towards Distributed Fiber Optic Sensor Commercialization

Work performed during Phase I unequivocally demonstrated that hydrazines could be reversibly detected using evanescent wave fiber optic sensor technology at sites where immobilized triphenylmethane dyes were present. Furthermore, currently commercially available electrooptical components were shown compatible with achieving a clear time delay as a consequence of the light pulse transmission time through the fiber optic cable. Future work will result in selecting optimum triphenylmethane dyes derivatized to the silica fiber optic for the reversible detection of trace hydrazines. This will be followed by optimization of electrooptic components for achieving a reliable distributed fiber optic sensor network for simultaneous multisite detection of trace hydrazine vapors in the atmosphere. Technology commercialization will then proceed following this stage.

Ensuring commercial success for distributed fiber optic sensor technology to emerge as a consequence of Phase I and II efforts depends in part on previous experience relating to fiber optic sensor product development, manufacturing and marketing. Towards this end Eltron is currently working towards commercial development of a multisite toxic gas detector system utilizing fiber optic signal transmission. We consider this to be our "first generation" fiber optic signal distributed sensor technology. This technology will be commercialized during performance of the Phase II program which will ensure rapid market entry for optimized "second generation" distributed fiber optic sensor technology to emerge towards the conclusion of the Phase II program.

First generation multi-point toxic gas detector system, currently under commercial development at Eltron, will include a home base unit providing access for up to eight chemical sensor inputs. This home base unit will include TTL/Relay alarm signals, simple data logging, and provide time-weighted-average (TWA), threshold limit values (TLV), lower explosive limits (LEL), and immediately dangerous to life or health (IDLH) signals. Communication with a host computer is through a serial interface such as RS232 or RS485. Current state of the art sensor heads are being used for the multi-point detection of a) carbon monoxide, b) hydrogen sulfide, c) ammonia, d) methane, e) propane, f) butane, g) ethylene, h) chlorine, i) nitrogen dioxide, j) ozone, and k) VOCs (volatile organic carbons). Output from sensor heads will be through a fiber optic link with the home base unit. Power for the sensor head will be provided by the home base unit for sensor heads located less than 200ft away from the home base unit and provided locally for sensor heads located greater than 200ft.

The sensor head circuit includes the following components:

- Driver circuitry for sensor.
- Signal conditioning circuitry to convert full range outputs of sensor to a 0 1 volt output range. The circuit has at least an offset trim and a gain trim. Also the possibility of a temperature compensation circuit may be needed.
- The 0 1 volt output range is converted to a pulse train through a V/F (AD654).
- Circuitry to convert the pulse train from the V/F into an optical pulse train suitable for transmitting the signal through a fiber-optic cable up to 500ft. Longer lengths will be

considered later.

• Power for the sensor head will be supplied through a cable going back to the "home unit" for distances of less than 200ft. Optionally the sensor head may be powered locally by a plug in adapter. The sensor head design currently being implemented is shown in Figure 35.

Key points in the home base unit (Figure 36) include the following:

- At least 8 pushbutton function keys.
- 8 rows of multiple LED's (green, yellow, and red for each sensor).
- LCD multiline display.
- TTL alarm signal for each of the 8 sensors.
- Small piezo speaker for audible alarm.
- Serial communications (RS232 or RS485).
   8 optical pulse converters (either photodiodes or phototransistors).
- Counting circuitry multiplexed to the 8 pulse signals.
- Microcontroller/microprocessor to control all functions.
- Power supply suitable to drive 8 sensor heads at up to 200ft away should be either built into the home base unit or a separate unit that sits under the home base unit.

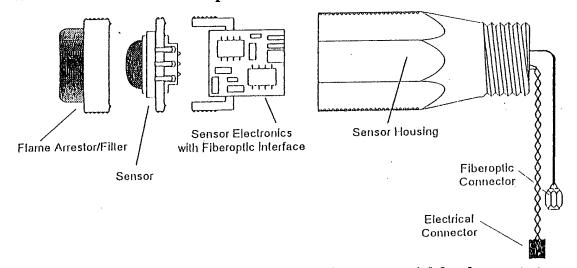


Figure 35. First generation sensor head design under commercial development at Eltron incorporating fiber optic signal transmission.

#### VIII. POTENTIAL POST APPLICATIONS

The proposed project will find application for the real time perimeter monitoring of hydrazines at missile launch sites and fighter aircraft used by the Air Force. This instru-

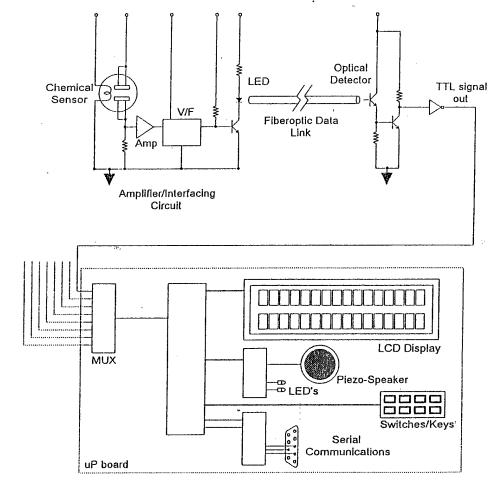


Figure 36. Schematic of fiber optic communication link strategy between sensor and home base unit for "first generation" technology currently being implemented at Eltron.

instrumentation technology will consequently be of potential utility by the Federal Government as the atmospheric exposure levels for hydrazines become more stringent. The capability for real time perimeter monitoring of toxic chemicals will have generic application in several industries where routine monitoring for leaks is mandated. Therefore, the technology under development here is expected to find broad based application in the private sector.

One commercial application where a distributed fiber optic chemical sensor network would find application is in the monitoring of Indoor Air Quality (IAQ). Because of energy conservation technologies, buildings, both office and industrial, are better sealed to the environment. This has led to what is commonly known as the "sick building syndrome." The Occupational Safety and Health Administration (OSHA) is addressing this problem through a series of regulations that will require the development of commercial buildings to have an adequate IAQ management plan. Although the issue is one of proper ventilation monitoring of particular species within a commercial building is used as a measure of the effectiveness of the ventilation system and therefore of the potential for a building to be a "sick building" with increased illnesses among its occupants.

Specific chemical species and parameters that cause "sick building syndrome" and

therefore are useful for gauging the effectiveness of commercial building ventilation systems include  $CO_2$ , CO, NO,  $SO_2$ ,  $O_3$ , radon, asbestos and formaldehyde. Physical parameters that are important include temperature and humidity. Of these species, the most important indicator of ventilation performance and most widely monitored today is  $CO_2$ . This is also relatively easy to monitor as opposed to the other chemical species listed above. Temperature and humidity are not only monitored but regulated as well and are also potential targets for monitoring IAQ.

To monitor CO<sub>2</sub>, several methods exist. However, for real time monitoring, NonDispersive InfraRed (NDIR) analyzers are the most common. These devices operate by measuring the absorption of CO<sub>2</sub> at a specific infrared wavelength. The intensity of this absorption peak is proportional to the CO<sub>2</sub> concentration. These instruments exist in a single-site monitoring mode. For the application of IAQ monitoring within a building, several sensors would be required to be dispersed throughout the building, including multiple stories. To achieve spatial monitoring using these current monitoring devices, tens, or even hundreds depending upon the size of the building, of individual sensors would be needed. Each individual sensor would be powered independently and would then need to be networked via an electrical system or other type of communication system to return the signals to a central station where building personnel would examine the results for problems in the building's ventilation system.

The advantage of a distributed fiber optic chemical sensor in this situation is that the networking, and therefore spatial monitoring, is done through the fiber optic system. Power at each individual sensor site would not be needed. Rather than having a set of electrooptics including the communications interface, at each site, the distributed fiber optic chemical sensor network has this communications feature already built in. This is expected to decrease complexity, reliability and cost of a fiber optic IAQ monitoring system relative to a NDIR-based system.

In addition to  $CO_2$ , temperature and humidity are important parameters for monitoring IAQ and can easily be monitored using fiber optics. There are currently commercially available fiber optic temperature sensors which could be adapted for use in IAQ monitoring. Although there are no fiber optic humidity sensors currently available that we are aware of, there has been a great deal of research in this area and these results can also be adapted into a commercial instrument.

Also of interest is monitoring formaldehyde as an indication of IAQ. Several methods are currently available, including colorimetric, for detecting formaldehyde. Although we are not aware of any commercially available fiber optic formaldehyde sensors, the chemistry involved in the colorimetric methods should be adaptable to a fiber optic sensor and therefore represents another potential analyte for determining IAQ.

The market for gas sensors is very diversified with applications in the automotive, petrochemical and chemical, power generation and building monitors. The types of sensors currently in use are also very diversified. Not all of these applications are targets for Eltron gas sensing technology. Currently, the worldwide market for fiber optic chemical sensors is small, estimated at \$14.5 million in 1993 and expected to grow at 5% per year reaching \$18 million by 1998. The reason for both the low absolute market size and low growth rate is the fact that this is a very new and still developing technology which has not been completely

accepted in the market. This will change over time.

A more realistic estimate for the potential market comes from looking at the overall gas sensor market, independent of the sensor technology. In the U.S., the industrial gas sensor market was \$329 million in 1992.<sup>19</sup> Of this market, 47%, or \$155 million, was in the automotive market alone.<sup>19</sup> This market is not a target for Eltron's gas sensing technology and therefore the potential market for Eltron technology is \$174 million. The overall market is estimated to grow at a compound annual rate of 15.5% leading to an estimated market of \$775 million in 1998.<sup>19</sup> Again, it is estimated that 60% of this market will be due to automotive applications and so is not a potential target for Eltron gas sensing technology.<sup>19</sup> This leaves a potential market of \$310 million by 1998.

#### VIII. REFERENCES

- 1. A.T. Varhanyan, Zhur. Fiz Khim, <u>35</u>, 2241 (1961).
- 2. A.T. Vartanyan, Russian J. Physical Chemistry, <u>36</u>, 1890 (1962).
- 3. A.T. Vartanyan, Russian J. Physical Chemistry, 36, 1142 (1962).
- 4. J.F. Giuliani and H. Wohltjen, U.S. Patent 4,513,087, April 23 (1985).
- 5. E.W. Schmidt, "Hydrazine and its Derivatives," John Wiley and Sons, New York, Chapt. 4 (1984).
- 6. Ibid., Chapt. 3.
- 7. W.R. Seitz, Anal. Chem., <u>56</u>, 16A (1984).
- 8. L.J. Luskus, "Measuring Hydrazine Vapor Concentrations in Air," 1981 JANNAF Safety and Environmental Protection Subcommittee, CPIA Publ. 348, 135 (1981).
- 9. H.N. Volltrauer and L.J. Luskus, "Breadboard Chemiluminescent Analyzer for Measurement of Hydrazines," Aerochem. Res. Labs T.P.-335 (1977).
- 10. J.R. Stetter, K.A. Tellefsen, R.A. Saunders and J.J. Decorpo, Talanta, 26, 799 (1979).
- 11. M.S. Abdel-Latif, Aisuleiman, G.G. Guilbault, B.A.A. Dromel and R.D. Schmid, Anal. Lett., 23, 375 (1990).
- 12. C. Klimcak, G. Radhakrishnan, S. Delcamp, Y. Chan, B. Jaduszliwer and S. Moss, SPIE Proc. Chem. Biochem. Env. Fiber Sensors VI, <u>2293</u>, 209 (1994).
- 13. C. Klimcak, G. Radhakrishnan and B. Jaduszliwer, SPIE Proc. Optical Sensors for Env. Chem. Proc. Monitoring, <u>2367</u>, 80 (1995).
- 14. O.S. Wolfbeis, ed., "Fiber Optic Chemical Sensors and Biosensors," CRC Press Florida, Volumes I, II (1990).
- 15. H. Zollinger, "Color Chemistry: Synthesis, Properties, and Applications of Organic Dyes and Pigments", VCH; New York, 1987; Ch. 4.
- 16. R. Kist, in "Optical Fiber Sensors: Systems and Applications," Vol. II, Culshaw, B. and Dakin, J. eds., Artech House, MA, Ch. 14 (1989).
- 17. R.P. Gaynor, Heating/Piping/Air Conditioning, Aug., 55 (1993).
- 18. BCC Market Research, "Fiber Optic Sensors," March 1994.
- 19. Frost & Sullivan, Inc., "U.S. Industrial Gas Sensor Markets," June 1994.